Phenomenological model of bacterial aerotaxis with a negative feedback[*]

Vladas Skakauskas[a,1]**, Pranas Katauskis**[a]**, Remigijus Šimkus**[b]**,
Feliksas Ivanauskas**[a]

[a]Faculty of Mathematics and Informatics, Vilnius University
LT-03225 Vilnius, Lithuania
vladas.skakauskas@maf.vu.lt; pranas.katauskis@mif.vu.lt; feliksas.ivanauskas@maf.vu.lt

[b]Vilnius University Institute of Biochemistry
LT-08662 Vilnius, Lithuania
simkus@bchi.lt

Abstract. A phenomenological model for the suspension of the aerotactic swimming micro-organisms placed in a chamber with its upper surface open to air is presented. The model was constructed to embody some complexity of the aerotaxis phenomenon, especially, changes in the average bacteria drift velocity under changing environmental conditions. It was assumed that effective forces applied to the cell (gravitational, drag, and thrust) should be essential for the overall system dynamics; and that bacterial propulsion force, but not their swimming velocity, is proportional to the gradient of the oxygen concentration. Mathematically, the model consists of three coupled equations for the oxygen dynamics; for the cell conservation; and for the balance of forces acting on bacteria. An analytical steady-state solution is given for the shallow and deep layers and numerical results are given for the steady-state and initial value problems which are compared with corresponding ones to the Keller–Segel model.

Keywords: bioconvection, thermo-bioconvection, swimming microorganisms, oxytactic bacteria.

1 Introduction

The term *aerotaxis* (or *oxytaxis*) refers to the situation where bacterium moves towards or away from air or oxygen. Aerotaxis can be regarded as a kind of the more general process, *chemotaxis*, which is a motion of bacteria towards a favorable chemical field. The basic mathematical model in chemotaxis was introduced by Keller and Segel (KS) [1, 2]. In its original form this model consists of four coupled reaction–advection–diffusion equations. Under the quasi-steady-state assumptions this model can be reduced to two coupled parabolic equations for the concentration of microorganisms and the attracting

---

[1]Corresponding author.

species (attractants). Mathematical modeling of chemotaxis on the basis of the KS model has developed into a large and diverse discipline [3, 4]. KS type equations were used to describe the oxytactic motion of bacteria in a water column as well [5–7]. Hillesdon, Pedley and Kessler (HPK) [6] and Hillesdon and Pedley (HP) [7] considered dynamics of an oxytactic bacteria Bacillus subtilis suspension placed in a chamber with its upper surface open to air. In the HPK model the phenomena of *gravitational sedimentation*, *bulk fluid motion*, and *diffusion of inactive cells* were assumed to be negligible. The assumption that the sedimentation rate is much smaller than the typical cell swimming speed is inaccurate in the case of inactive cells [7]. The typical form of the KS model for the oxytactic bacteria is [5–7]:

$$
\begin{cases}
\dfrac{\partial C}{\partial t} = \mathrm{div}(\kappa_1 \nabla C) - \kappa_2(C)B, \\[2mm]
\dfrac{\partial B}{\partial t} = \mathrm{div}\big(-\kappa_3(C)B\nabla C + \kappa_4(C)\nabla B\big).
\end{cases}
\tag{1}
$$

Here C and B are the oxygen and cells concentrations, κ_1 and $\kappa_4(C)$ are the diffusivity of oxygen and bacterial cells, $\kappa_2(C)$ is the oxygen consumption rate by cells, $v = \kappa_3(C)\nabla C$ is the oxytactic bacteria drift velocity, $\kappa_3(C)$ is the oxytactic sensitivity, ∇ and div are the gradient and divergence operators. In the steady-state, wide chamber, and constant $\kappa_1, \ldots, \kappa_4$ case, HPK gave an analytic solution of the model for both shallow and deep chambers. In the deep chamber case, the authors neglected diffusion of inactive cells and therefore one constant was not determined. This constant was obtained by numerically solving the initial value problem. In the time-dependent one-dimensional case with constant κ_1 and depending on C coefficients κ_2, κ_3, and κ_4, HPK solved model (1) numerically using the method of lines. HP examined the stability of the steady-state solution.

To describe the convective chemotaxis Dombrowski et al. [8], Tuval et al. [9] generalized the KS model by including the bulk fluid motion. This model describes the collective behavior (bioconvection) of a suspension of oxytactic bacteria in an incompressible fluid under assumptions [10] that the contribution of bacteria to the bacteria–fluid suspension is sufficiently small and that more detailed cell–cell interactions (e.g., of hydrodynamic type) are neglected. In [10], this model was studied numerically in detail. The solvability of the model was examined by Lorz [11], Duan et al. [12], and Di Francesco et al. [13]. Becker et al. [14] and Kuznetsov [15, 16] generalized the KS model and studied the bioconvection of oxytactic cells in a fluid saturated porous medium. Kuznetsov also investigated models for the thermo-bioconvection of oxytactic cells in a fluid layer [17–19] and in a fluid saturated porous layer [15, 16] and carried out the stability analysis of their steady-state solutions. In all models of bioconvection and thermo-bioconvection, the oxytactic bacteria drift velocity, as in the KS model, is proportional to the gradient of oxygen concentration while the gravitational force is approximated by the buoyancy term. Papers of Alloui et al. [20, 21] are devoted to numerical study of the development of gravitactic bioconvection and thermo-bioconvection of swimming microorganisms which are little denser than water and move randomly, but on the average, upwardly against

gravity. Alloui et al. [22] also carried out the linear stability analysis of the thermo-bioconvection of swimming against gravity microorganisms.

We note three problems that arise in mathematical modeling of bacterial aerotaxis. *Firstly*, it should be noted, that an important aspect of KS chemotaxis models is the expected onset of chemotactic collapse [3, 4, 23]. This term refers to the fact that, under suitable circumstances, the whole population should concentrate in a single point in finite time. However, it seems likely, that real bacterium is searching for the optimal place to be. Therefore, the overcrowding of bacteria in small space domains is unrealistic due to lack of nutrition for population in this domain. A number of modifications have been made to the minimal KS model of auto-aggregation that allows preventing such unrealistic singularities [4]. In general, this means, that in real systems there are certain dispersal mechanisms, which can be regarded as a negative chemotaxis and/or the suppression of the positive chemotaxis. The corresponding dispersal mechanisms were not taken into account in the KS type models of aerotaxis. *Secondly*, in real systems, the response of microorganisms to oxygen is much more complicated than the simplest KS model suggests [24–27]. It is known, that dependently on the type of bacteria and local environmental conditions, oxygen can act as an attractant or as a repellent ([24,25] and references therein). The positive aerotaxis (oxygen is attractant) results in aggregation of cells at the oxygen-exposed surfaces and the negative aerotaxis (oxygen is repellent) imply dispersal of the cell. Thus, again, a certain mechanism of the suppression of the positive aerotaxis should be included to the overall dynamic system. *Thirdly*, a common feature of many chemotaxis models based on the approximation of the cells drift velocity by the gradient of the chemoattractant or chemorepellent is to incorporate some complexity of the chemotaxis into the equations through a chemotactic sensitivity function (see system (1)). But different microorganisms detect spatial gradients of the chemical signal through distinct mechanisms. Certain cells [28], such as *Dystyostelium discoideum*, fibroblasts and leukocytes, can detect and respond to a small gradient in the chemical signal across the length of their body using a process of internal amplification and polarisation. Smaller cells [29], such as *E. coli*, detect a gradient by sampling the concentration at different time points and modifying their movement accordingly. The observation that the gradient sensed by bacteria is temporal means that bacteria possess a memory, which compares past information with present information to make a decision. This memory is long enough so that the bacteria can make an accurate comparison between two points more distal than the bacterial body length. In both cases, the signal detected by the cell is intrinsically *non-local* and it may therefore be appropriate to consider movement based on *non-local gradient* by the integration of the signal by the cell over some region. For cells which detect a gradient in the chemical signal across the length of their body, Othmer and Hillen [30] approximated their drift velocity by the formula $\chi Cn/(\omega\rho) \int_{S^{n-1}} \sigma B(t, x + \rho\sigma) \, d\sigma$ where $\omega = |S^{n-1}|$, S^{n-1} denotes the $(n-1)$-dimensional unit sphere in $\mathbb{R}^n$, and ρ is the radius of a sphere which enclose the cell. Analytical and numerical study of this model is given in [31]. Studies of smaller cells revealed (see [28] and literature therein) that, like many other sensory systems, the chemotactic response involves two processes: excitation and adaptation. When bacteria are stimulated, their swimming mode are changed instantaneously. This initial process, termed excitation, is very fast. Later on,

bacteria resume their prestimulus behaviour, even though the stimulus is still present. This process, termed adaptation, is relatively slow (in the range of seconds or minutes). Adaptation thus enable bacteria to adjust to changes in the stimulus intensity and respond to new stimuli. Models of KS type are based on the quasi-steady-state approximation of the cells drift velocity and therefore cannot describe correctly the adaptation period.

The aim of this paper is study of the dynamics of the dilute suspensions of aerotactic bacteria by the modified KS model. To describe some complexity of the aerotaxis phenomenon (especially, the bacteria adaptation period under changes in environmental conditions), we replace the quasi-steady-state equation $v = \kappa_3(C)\nabla C$ by the momentum equation for cells drift velocity. In the modified model it is assumed that 1) gravitational, drag, and thrust forces applied to the cell are not negligible and 2) that bacterial thrust force, but not its average drift velocity, is proportional to the gradient of the oxygen concentration. The model consists of three coupled equations: 1) the equations for oxygen dynamics; 2) cell conservation equation; and 3) momentum equation for the cells drift velocity. This original model of oxytaxis is termed as FB (Feedback/Force balance) model. In the wide chamber case, we give an analytic solution of the model for both shallow and deep chambers and discuss the numerical results of the initial value and steady-state problems. We also solved the KS model and using numerical results demonstrate difference between the FB and KS models.

The paper is organized as follows. In the auxiliary Section 2, we introduce the KS model and give a detail derivation of its steady-state solution found by HPK. In Section 3, we present the FB model and demonstrate its steady-state solution. In Section 4, we compare numerical results for the KS and FB models. Some remarks in Section 5 conclude the paper.

2 The one-dimensional Keller–Segel (KS) model

In this auxiliary section, we introduce the KS model and give a detail derivation of its steady-state solution which was found by HPK [6]. Let x be the vertical coordinate. In the one-dimensional case, Eqs. (1) can be written in the form

$$
\begin{cases}
\dfrac{\partial C}{\partial t} = \dfrac{\partial}{\partial x}\left(\kappa_1 \dfrac{\partial C}{\partial x}\right) - \kappa_2(C)B, & x \in (0, h), \\[2ex]
\dfrac{\partial B}{\partial t} = \dfrac{\partial}{\partial x}\left(-\kappa_3(C)B\dfrac{\partial C}{\partial x} + \kappa_4(C)\dfrac{\partial B}{\partial x}\right), & x \in (0, h),
\end{cases}
\tag{2}
$$

$$
\begin{cases}
C(0, x) = C_0, \quad B(0, x) = B_0, \quad C(t, h) = C_0, \\[2ex]
\left.\dfrac{\partial C}{\partial x}\right|_{x=0} = \left.\dfrac{\partial B}{\partial x}\right|_{x=0} = 0, \\[2ex]
\left.\left(\kappa_3(C)B\dfrac{\partial C}{\partial x} - \kappa_4(C)\dfrac{\partial B}{\partial x}\right)\right|_{x=h} = 0.
\end{cases}
\tag{3}
$$

Here $x = 0$ and $x = h$ correspond to the bottom and surface of the chamber, the constant C_0 is the initial and atmosphere oxygen concentration, B_0 is the initial cells concentration. The total number of cells is equal to the hB_0.

Now we introduce the dimensionless variables. Set $\Theta = (C - C_{\min})/(C_0 - C_{\min})$, where $C_{\min}$ is the minimal value of the oxygen concentration necessary for cells to be active. Let $\kappa_2(C) = \kappa_{20}w_2(\Theta)$, $\kappa_3(C) = \kappa_{30}w_3(\Theta)$, $\kappa_4(C) = \kappa_{40}w_4(\Theta)$, with constants κ_{20}, κ_{30}, and κ_{40}. Assuming that κ_1 is also constant HPK considered the case where $w_2 = w_3$, $w_4 = w_2^2$, with w_2 the Heaviside step function. Set $x = h\bar{x}$, $B = B_0\bar{B}$, $t = (h^2/\kappa_{40})\bar{t}$. Omitting the bar, we rewrite (2), (3) in the dimensionless form

$$
\begin{cases}
\dfrac{\partial \Theta}{\partial t} = \delta\left(\dfrac{\partial^2 \Theta}{\partial x^2} - \beta^2 w_2(\Theta)B\right), \quad x \in (0,1), \\[2mm]
\dfrac{\partial B}{\partial t} = \dfrac{\partial}{\partial x}\left(w_4(\Theta)\dfrac{\partial B}{\partial x} - \alpha w_3(\Theta)B\dfrac{\partial \Theta}{\partial x}\right), \quad x \in (0,1), \\[2mm]
\left.\dfrac{\partial \Theta}{\partial x}\right|_{x=0} = \left.\dfrac{\partial B}{\partial x}\right|_{x=0} = 0, \\[2mm]
\left(w_4(\Theta)\dfrac{\partial B}{\partial x} - \alpha w_3(\Theta)B\dfrac{\partial \Theta}{\partial x}\right)\bigg|_{x=1} = 0, \\[2mm]
\Theta(t,1) = 1, \\[1mm]
B(0,x) = \Theta(0,x) = 1,
\end{cases}
\tag{4}
$$

where $\delta = \kappa_1/\kappa_{40}$, $\beta^2 = B_0\kappa_{20}h^2/(\kappa_1(C_0 - C_{\min}))$, $\alpha = \kappa_{30}(C_0 - C_{\min})/\kappa_{40}$. Note that α is swimming upwards parameter. Integrating over $(0,1)$ Eq. $(4)_2$ and using conditions $(4)_{3,4}$, we get that $\int_0^1 B(t,x)\,\mathrm{d}x = 1$ is preserved. In the steady-state case, system (4) reads

$$
\begin{cases}
\Theta'' = \beta^2 w_2(\Theta)B, \\[1mm]
\left(w_4(\Theta)B' - \alpha w_3(\Theta)B\Theta'\right)' = 0, \\[1mm]
\Theta(1) = 1, \\[1mm]
w_4(1)B'(1) - \alpha w_3(1)B(1)\Theta'(1) = 0, \\[1mm]
\Theta'(0) = B'(0) = 0.
\end{cases}
\tag{5}
$$

In addition, we formulate the condition

$$
\int\limits_0^1 B(x)\,\mathrm{d}x = 1.
\tag{6}
$$

Now we derive the HPK steady-state solution of system (5) and (6).

2.1   The shallow layer case ($\Theta > 0 \ \forall x \in (0,1]$)

Integrating $(5)_2$ and using condition $(5)_4$ we get the equation

$$
w_4(\Theta)B' = \alpha w_3(\Theta)B\Theta'.
\tag{7}
$$

In this section, we consider the case $w_2 = w_3 = w_4 = 1$. From $(5)_1$ and (7) we get the equation $B' = \alpha\beta^{-2}\theta'\theta''$ which has the solution $B = (\alpha/2)\beta^{-2}(\theta')^2 + B(0)$. Hence,

$$\Theta' = \beta\sqrt{\frac{2}{\alpha}}\,\sqrt{B - B(0)}. \tag{8}$$

From (7) and (8) we derive the equation

$$B' = \alpha\beta B\sqrt{\frac{2}{\alpha}\big(B - B(0)\big)}$$

which has the solution

$$B = B(0)\cos^{-2}(\xi x), \quad \xi = \beta\sqrt{\frac{\alpha B(0)}{2}} \in \left(0, \frac{\pi}{2}\right). \tag{9}$$

Then combining (8) and (9) we get

$$\Theta' = \frac{2}{\alpha}\xi\tan(\xi x), \qquad \Theta(1) = 1.$$

Hence

$$\Theta = 1 - \frac{2}{\alpha}\ln\frac{\cos(\xi x)}{\cos\xi}. \tag{10}$$

Since Θ must be nonnegative the condition $\cos(\xi x)/\cos\xi \leqslant e^{\alpha/2}$ has to be satisfied for all $x \in [0, 1]$. Hence $\cos\xi \geqslant e^{-\alpha/2}$ or $\cos^{-2}\xi \leqslant e^{\alpha}$ and $0 \leqslant \xi \leqslant \arccos e^{-\alpha/2}$. From condition (6) and Eq. (9) we get the equation

$$\frac{q}{\xi} = \tan\xi, \tag{11}$$

where $q = \alpha\beta^2/2$. Eq. (11) has a unique solution $\xi = \xi(q) \in (0, \arccos e^{-\alpha/2})$ growing together with q since $\mathrm{d}\xi/\mathrm{d}q > 0$. Then, from Eqs. $(9)_2$ and (11) it follows that $B(0) = \xi^2(q)/q$ and $\cos^{-2}\xi(q) = 1 + \tan^2\xi(q) = 1 + q^2/\xi^2(q) \leqslant e^{\alpha}$. Thus $\arccos e^{-\alpha/2} \geqslant \xi(q) \geqslant q/\sqrt{e^{\alpha} - 1} = \alpha\beta^2/(2\sqrt{e^{\alpha} - 1})$ and, hence,

$$\beta^2 \leqslant \beta_*^2 = \frac{2}{\alpha}\sqrt{e^{\alpha} - 1}\,\arccos e^{-\alpha/2}. \tag{12}$$

Thus $\theta(0) > 0$ if $0 < \beta < \beta_*$, and $\theta(0) = 0$ if $\beta = \beta_*$. Values of β that satisfy the inequality $\beta \leqslant \beta_*$ correspond to a shallow chamber. All others correspond to a deep chamber. Note that $\partial\Theta/\partial q = (2/\alpha)(-\tan\xi + x\tan x\xi)\,\mathrm{d}\xi/\mathrm{d}q < 0 \;\forall x \in (0, 1)$.

2.2   The deep layer case

In this case $\beta > \beta_*$ and positive Θ determined by Eq. (10) does not exist for all $x \in [0, 1]$. Θ is positive in a layer $(x_*, 1]$, $\Theta(x_*) = 0$, where $x_* > 0$ is unknown a priori. There is not

enough oxygen available in the layer $[0, x_*]$ and cells are inactive. Therefore $w_2(\Theta) = 0$ and we have to consider the task $\Theta'' = 0$, $\Theta'(0) = \Theta(x_*) = 0$. Hence, $\Theta = 0$ for all $x \in [0, x_*]$. Independently of w_3 and w_4 from (7) it follows that $B(x) = B(x_*)$ $\forall x \in [0, x_*]$, where $B(x_*)$ is also unknown a priori.

HPK neglected diffusion of inactive cells and therefore $B(x_*)$ was not determined by the conditions of the steady-state case. HPK determined it by solving the initial value problem. Differently from HPK, we *postulate the continuity* of B and B' at x_*. We also use the continuity condition for Θ and Θ' at x_*. In $(x_*, 1]$ we have to solve Eqs. (5)$_{1,2,3,4}$ and (6). Let $w_2 = w_3 = w_4 = 1$. By the argument used for the shallow chamber and by the continuity conditions at x_* we get

$$\begin{cases} B = B(x_*) \cos^{-2}\big(\tilde{\xi}(x - x_*)\big), \quad \tilde{\xi} = \beta \sqrt{\dfrac{\alpha B(x_*)}{2}}, \\ \Theta = 1 - \dfrac{2}{\alpha} \ln \dfrac{\cos(\tilde{\xi}(x - x_*))}{\cos(\tilde{\xi}(1 - x_*))} > 0 \end{cases} \tag{13}$$

for $x \in (x_*, 1]$ and $(1 - x_*)\tilde{\xi} \in (0, \pi/2)$. Due to the condition $\Theta(x_*) = 0$ it follows that $-\alpha/2 = \ln \cos(\tilde{\xi}(1 - x_*))$. Hence

$$\tan\big(\tilde{\xi}(1 - x_*)\big) = \sqrt{e^\alpha - 1}. \tag{14}$$

At last, from condition (6) we get

$$1 = B(x_*)x_* + \int\limits_{x_*}^{1} B(x)\,\mathrm{d}x = B(x_*)\bigg(x_* + \dfrac{1}{\tilde{\xi}\tan(\tilde{\xi}(1 - x_*))}\bigg). \tag{15}$$

Combining the last two equations and using the definition of $\tilde{\xi}$ we get the equation

$$1 = \dfrac{2\tilde{\xi}^2}{\alpha\beta^2}\bigg(x_* + \dfrac{\sqrt{e^\alpha - 1}}{\tilde{\xi}}\bigg)$$

which has the solution

$$\tilde{\xi} = \dfrac{\sqrt{e^\alpha - 1 + 2x_*\alpha\beta^2} - \sqrt{e^\alpha - 1}}{2x_*}. \tag{16}$$

Now from (14) it follows that $(1 - x_*)\tilde{\xi} = \eta(\alpha) := \arccos e^{-\alpha/2}$. Hence,

$$\dfrac{1 - x_*}{2x_*}\big(\sqrt{e^\alpha - 1 + 2x_*\alpha\beta^2} - \sqrt{e^\alpha - 1}\big) = \eta(\alpha).$$

This equation has the solution

$$x_* = 1 - \eta\dfrac{\sqrt{(\eta - \sqrt{e^\alpha - 1})^2 + 2\alpha\beta^2} - (\eta - \sqrt{e^\alpha - 1})}{\alpha\beta^2} \in (0, 1) \tag{17}$$

such that $\mathrm{d}x_*/\mathrm{d}\beta > 0$. Combining (16) and (17) we derive an equation for $\tilde{\xi}$ and then from (15) get an equation for $B(x_*)$:

$$
\begin{cases}
\tilde{\xi} = \dfrac{\alpha\beta^2}{\sqrt{(\eta - \sqrt{\mathrm{e}^\alpha - 1})^2 + 2\alpha\beta^2} - (\eta - \sqrt{\mathrm{e}^\alpha - 1})} > 0, \\[4mm]
B(x_*) = \dfrac{2\alpha\beta^2}{[\sqrt{(\eta - \sqrt{\mathrm{e}^\alpha - 1})^2 + 2\alpha\beta^2} - (\eta - \sqrt{\mathrm{e}^\alpha - 1})]^2}.
\end{cases}
\tag{18}
$$

We see that the steady-state solution does not depend on the positive diffusivity of inactive cells.

In Section 4, we give the numerical solution of the initial value problem (4) determined by using the finite-difference scheme.

3 The feedback/force balance (FB) model

Keller and Segel neglected the bulk fluid velocity and approximated the average velocity of swimming upwards oxytactic bacteria by the quasi steady-state formula $v = \kappa_3(C)\nabla C$. We also neglect the bulk fluid motion but, to describe some complexity of the aerotaxis phenomenon (especially, the bacteria adaptation period under changes in environmental conditions), we use the momentum equation for cells which includes the gravitational sedimentation of cells, swimming upwardly strength (force which arises from chemotaxis and enables cells to swim), and resistance force to movement of cells through the fluid. We postulate that swimming upwards strength of cells, but not their average velocity, is parallel and proportional to ∇C. For simplicity, we neglect the bacteria to bacteria communication and convective acceleration, $(v \cdot \nabla)v$, terms in the momentum equation for cells. In the one-dimensional case, the model consists of the equations

$$
\begin{cases}
\dfrac{\partial C}{\partial t} = \dfrac{\partial}{\partial x}\left(\kappa_1 \dfrac{\partial C}{\partial x}\right) - \kappa_2(C)B, & x \in (0, h), \\[3mm]
\dfrac{\partial B}{\partial t} = \dfrac{\partial}{\partial x}\left(-Bv + \kappa_4(C)\dfrac{\partial B}{\partial x}\right), & x \in (0, h), \\[3mm]
B\dfrac{\partial v}{\partial t} = -B\tilde{g} - \kappa_5(C)v + \tilde{\kappa}_3(C)\dfrac{\partial C}{\partial x}, & x \in (0, h),
\end{cases}
\tag{19}
$$

subject to the conditions

$$
\begin{cases}
C(0, x) = C_0, & B(0, x) = B_0, & v(0, x) = v_0, \\[2mm]
C(t, h) = C_0, & \dfrac{\partial C}{\partial x}\bigg|_{x=0} = 0, \\[2mm]
\left(Bv - \kappa_4(C)\dfrac{\partial B}{\partial x}\right)\bigg|_{x=0;h} = 0.
\end{cases}
\tag{20}
$$

Here $\kappa_1 = \mathrm{const}$, $\tilde{g} = g(1 - \rho_w/\rho_B)$ where g is the acceleration due to the gravity, ρ_w and ρ_B are the water (fluid) and a cell density. Note that the dimensions of κ_3 in Section 2

and $\tilde{\kappa}_3$ in Section 3 are different. Integrating Eq. (19)$_3$ we get a non-local in time equation for average cells drift velocity v,

$$v(t,x) = v_0(x)\Pi(0,t,x) + \int_0^t \left(-B(\xi,x)\tilde{g} + \tilde{\kappa}_3\big(C(\xi,x)\big)\frac{\partial C(\xi,x)}{\partial x} \right)\Pi(\xi,t,x)\,\mathrm{d}\xi$$

where $\Pi(\xi,t,x) = \exp\{-\int_\xi^t \kappa_5(C(\tau,x))\,\mathrm{d}\tau\}$.

Let $\kappa_2(C) = \kappa_{20}w_2(\Theta)$, $\tilde{\kappa}_3(C) = \tilde{\kappa}_{30}w_3(\Theta)$, $\kappa_4(C) = \kappa_{40}w_4(\Theta)$, $\kappa_5(C) = \kappa_{50}w_5(\Theta)$, $\Theta = (C - C_{\min})/(C_0 - C_{\min})$, $x = \bar{x}h$, $B = B_0\bar{B}$, $t = (h^2/\kappa_{40})\bar{t}$, $v = v_*\bar{v}$. Omitting the bar we rewrite system (19) and (20) in the dimensionless form

$$\begin{cases} \dfrac{\partial \Theta}{\partial t} = \delta\left(\dfrac{\partial^2 \Theta}{\partial x^2} - \beta^2 w_2(\Theta)B \right), \quad x \in (0,1), \\[2mm] \dfrac{\partial B}{\partial t} = \dfrac{\partial}{\partial x}\left(w_4(\Theta)\dfrac{\partial B}{\partial x} - \gamma Bv \right), \quad x \in (0,1), \\[2mm] B\dfrac{\partial v}{\partial t} = -\rho_1 B - \rho_3 w_5(\Theta)v + \rho_2 w_3(\Theta)\dfrac{\partial \Theta}{\partial x}, \quad x \in (0,1), \end{cases} \tag{21}$$

$$\begin{cases} \Theta(0,x) = 1, \quad B(0,x) = 1, \quad v(0,x) = v_0, \\[2mm] \dfrac{\partial \Theta}{\partial x}\bigg|_{x=0} = 0, \quad \Theta|_{x=1} = 1, \\[2mm] \left(w_4(\Theta)\dfrac{\partial B}{\partial x} - \gamma vB \right)\bigg|_{x=0;1} = 0. \end{cases} \tag{22}$$

Here $\delta = \kappa_1/\kappa_{40}$, $\gamma = v_*h/\kappa_{40}$, $\beta^2 = B_0\kappa_{20}h^2/(\kappa_1(C_0 - C_{\min}))$, $\rho_1 = \tilde{g}h^2/(\kappa_{40}v_*) = \tilde{g}h^3/(\gamma\kappa_{40}^2)$, $\rho_2 = \tilde{\kappa}_{30}h(C_0 - C_{\min})/(v_*B_0\kappa_{40})$, $\rho_3 = h^2\kappa_{50}/(B_0\kappa_{40})$.

Note, that model (21)–(22) preserves condition $\int_0^1 B(t,x)\,\mathrm{d}x = 1$. Determining $a_1 = \rho_1\gamma/\rho_3$ and $a_2 = \rho_2\gamma/\rho_3$ we rewrite Eq. (21)$_3$ in the form

$$B\frac{\partial v}{\partial t} = \frac{\rho_3}{\gamma}\left(-a_1 B - \gamma\omega_5(\Theta)v + a_2\omega_3(\Theta)\frac{\partial \Theta}{\partial x} \right).$$

Now we consider the steady-state case.

3.1 The shallow chamber case ($\Theta > 0 \ \forall x \in (0,1]$)

We study the case where $w_2(\Theta) = w_3(\Theta) = w_4(\Theta) = w_5(\Theta) = 1$. From Eqs. (21) and (22) we get

$$\begin{cases} \Theta'' = \beta^2 B, \\[1mm] \gamma vB = B', \\[1mm] v = \dfrac{1}{\rho_3}(\rho_2\Theta' - \rho_1 B) = \dfrac{a_2}{\gamma}\Theta' - \dfrac{a_1}{\gamma}B, \\[1mm] \Theta'(0) = 0, \quad \Theta(1) = 1. \end{cases} \tag{23}$$

In addition, we formulate the condition

$$\int\limits_0^1 B(x)\,\mathrm{d}x = 1. \tag{24}$$

Integrating $(23)_1$ and using (24) we get

$$\Theta'(1) = \beta^2. \tag{25}$$

Then from Eqs. $(23)_{1,2,3}$ it follows that

$$\gamma v = \frac{B'}{B} = \beta^2 \frac{\mathrm{d}B}{\mathrm{d}\Theta'} = a_2\Theta' - a_1 B. \tag{26}$$

The last equation of (26) is linear and integrates to get

$$B(x) = \hat{B}\big(\Theta', B(0)\big) = \left(B(0) + \frac{a_2}{a_1^2}\beta^2\right)\exp\left(-\frac{a_1}{\beta^2}\Theta'\right) + \frac{a_2}{a_1}\Theta' - \frac{a_2}{a_1^2}\beta^2. \tag{27}$$

From (26) we can see that $v = 0$ and $\mathrm{d}B/\mathrm{d}\Theta' = 0$ at $B = (\rho_2/\rho_1)\Theta'$. Now, inserting this value of B into (27), we get

$$\Theta' = \frac{\beta^2}{a_1}\ln\left(1 + \frac{B(0)a_1^2}{a_2\beta^2}\right). \tag{28}$$

Then from (26) and $(23)_1$ it follows that

$$\begin{aligned}
B''|_{B=\frac{\rho_2}{\rho_1}\Theta'} &= \left\{B'\frac{\gamma}{\rho_3}(\rho_2\Theta' - \rho_1 B) + B\frac{\gamma}{\rho_3}(\rho_2\Theta'' - \rho_1 B')\right\}\bigg|_{B=(\rho_2/\rho_1)\Theta'} \\
&= B^2\frac{\rho_2}{\rho_3}\gamma\beta^2 > 0.
\end{aligned}$$

Hence, (28) is the point of a minimum of B and

$$\min B = \frac{\rho_2}{\rho_1}\frac{\beta^2}{a_1}\ln\left(1 + \frac{a_1^2 B(0)}{a_2\beta^2}\right) > 0.$$

We integrate Eqs. $(23)_1$ and (27) and use condition $(23)_4$ to get

$$\beta^2 x = \hat{x}\big(\Theta', B(0)\big) := \int\limits_0^{\Theta'} \frac{\mathrm{d}y}{\hat{B}(y, B(0))}. \tag{29}$$

From here and by (25) we get the equation for $B(0)$,

$$\beta^2 = \int\limits_0^{\beta^2} \frac{\mathrm{d}y}{\hat{B}(y, B(0))}. \tag{30}$$

After this equation is solved for $B(0)$, we determine $B = \hat{B}(\Theta', B(0))$ by Eq. (27), $x = \hat{x}(\Theta', B(0))$ by Eq. (29), and v by (23)$_3$ for $\Theta' \in [0, \beta^2]$.

At last, using (29) we integrate the equation $d\Theta = \Theta' \, \mathrm{d}x$ to get

$$\Theta = 1 - \frac{1}{\beta^2} \int_{\Theta'}^{\beta^2} \frac{y \, \mathrm{d}y}{\hat{B}(y, B(0))}. \tag{31}$$

This formula shows that $\Theta \geqslant 0$ for all $x \in [0, 1]$ if

$$\beta^2 \leqslant \tilde{\beta}_*^2 := \int_0^{\tilde{\beta}_*^2} \frac{y \, \mathrm{d}y}{\hat{B}(y, B(0))}. \tag{32}$$

Values β that satisfy condition $\beta \leqslant \tilde{\beta}_*$ correspond to shallow chamber. Substituting $y = \tilde{\beta}_*^2 z$, $B(0) = \tilde{\beta}_*^2 \tilde{B}(0)$ we rewrite Eqs. (30) and (31) in the form

$$\tilde{\beta}_*^2 = \int_0^1 \frac{\mathrm{d}z}{\tilde{B}(z, \tilde{B}(0))}, \qquad 1 = \int_0^1 \frac{z \, \mathrm{d}z}{\tilde{B}(z, \tilde{B}(0))}, \tag{33}$$

where $\tilde{B}(z, \tilde{B}(0)) = (\tilde{B}(0) + a_2/a_1^2) \exp(-a_1 z) + a_2 z/a_1 - a_2/a_1^2$.

From (33)$_2$ we determine $\tilde{B}(0)$ and then by (33)$_1$ find $\tilde{\beta}_*^2$. Clearly, $\tilde{\beta}_*^2 > 1$.

3.2 The deep chamber case ($\beta > \tilde{\beta}_*$)

Since function (31) is not positive for all $x > 0$, we divide $(0, 1]$ into two intervals $(0, \tilde{x}_*]$ and $(\tilde{x}_*, 1]$, $\Theta(\tilde{x}_*) = 0$. In $(\tilde{x}_*, 1]$, $\Theta > 0$, and cells consume oxygen and are active. Since $\Theta(\tilde{x}_*) = 0$, there is not enough oxygen available in $(0, \tilde{x}_*)$. Hence, cells are inactive and therefore $\kappa_2(\Theta) = 0 \; \forall x \in [0, \tilde{x}_*]$. Thus in $(0, \tilde{x}_*)$ we have the system

$$\begin{cases} \Theta'' = 0, \quad \Theta(\tilde{x}_*) = 0, \quad \Theta'(0) = 0, \\ \gamma v B = w_4(\Theta) B', \\ v = \dfrac{1}{\rho_3 w_5(\Theta)} \big(\rho_2 \omega_3(\Theta) \Theta' - \rho_1 B\big). \end{cases}$$

It is easy to see that $\Theta = 0$, $v = -\rho_1 B/(\rho_3 w_5(\Theta)) < 0$, $B' = -qB^2$, $q = \gamma \rho_1 / (\rho_3 w_4(0) w_5(0)) \; \forall x \in (0, \tilde{x}_*)$. Therefore

$$B(x) = \frac{B(\tilde{x}_*)}{1 - qB(\tilde{x}_*)(\tilde{x}_* - x)} = \frac{B(0)}{1 + qxB(0)}. \tag{34}$$

In $(\tilde{x}_*, 1)$, we consider the case $w_2 = w_3 = w_4 = w_5 = 1$, and solve Eqs. (23) with conditions $\Theta(1) = 1$, $\Theta(\tilde{x}_*) = \Theta'(\tilde{x}_*) = 0$. By the argument used for the shallow

chamber we get

$$
\begin{cases}
x - \tilde{x}_* = \dfrac{1}{\beta^2} \displaystyle\int\limits_0^{\Theta'} \dfrac{\mathrm{d}y}{\hat{B}(y, B(\tilde{x}_*))}, \\[2ex]
\Theta = 1 - \dfrac{1}{\beta^2} \displaystyle\int\limits_{\Theta'}^{\Theta'(1)} \dfrac{y\,\mathrm{d}y}{\hat{B}(y, B(\tilde{x}_*))}, \\[2ex]
B(x) = \hat{B}\big(\Theta', B(\tilde{x}_*)\big),
\end{cases}
\tag{35}
$$

where

$$
\hat{B}\big(\Theta', B(\tilde{x}_*)\big) = \left(B(\tilde{x}_*) + \frac{a_2}{a_1^2}\beta^2 \right) \exp\left(-\frac{a_1}{\beta^2}\Theta' \right) + \frac{a_2}{a_1}\Theta' - \frac{a_2}{a_1^2}\beta^2.
$$

From condition (24) by Eqs. (23)$_1$ and (34) we derive the equation

$$
\begin{aligned}
1 &= \int_0^{\tilde{x}_*} B\,\mathrm{d}x + \frac{1}{\beta^2}\int_{\tilde{x}_*}^1 \Theta''\,\mathrm{d}x = \frac{1}{\beta^2}\Theta'(1) + B(0)\int_0^{x_*} \frac{\mathrm{d}x}{1 + a_1 x B(0)} \\
&= \frac{1}{\beta^2}\Theta'(1) + \frac{1}{a_1}\ln\big(1 + a_1\tilde{x}_* B(0)\big) = \frac{1}{\beta^2}\Theta'(1) - \frac{1}{a_1}\ln\big(1 - a_1\tilde{x}_* B(\tilde{x}_*)\big).
\end{aligned}
$$

Hence,

$$
\begin{aligned}
\Theta'(1) &= \beta^2 u\big(\tilde{x}_*, B(\tilde{x}_*)\big), \\
u\big(\tilde{x}_*, B(\tilde{x}_*)\big) &= 1 + \frac{1}{a_1}\ln\big(1 - a_1\tilde{x}_* B(\tilde{x}_*)\big) \geqslant 0
\end{aligned}
\tag{36}
$$

provided that $B(\tilde{x}_*) < (1 - \mathrm{e}^{-a_1})/(a_1\tilde{x}_*)$. Inserting $x = 1$, $\Theta'(\tilde{x}_*)$ determined by (36) into Eq. (35)$_1$ and $\Theta(\tilde{x}_*) = 0$, $\Theta'(\tilde{x}_*)$ from (36) into Eq. (35)$_2$ we get

$$
\beta^2 = \int_0^{\beta^2 u(\tilde{x}_*, B(\tilde{x}_*))} \frac{y\,\mathrm{d}y}{\hat{B}(y, B(\tilde{x}_*))}, \qquad 1 - \tilde{x}_* = \frac{1}{\beta^2}\int_0^{\beta^2 u(\tilde{x}_*, B(\tilde{x}_*))} \frac{\mathrm{d}y}{\hat{B}(y, B(\tilde{x}_*))},
$$

which by substitution $y = \beta^2 u(\tilde{x}_*, B(\tilde{x}_*))\xi$ can be transformed into

$$
\begin{cases}
1 - \tilde{x}_* = \displaystyle\int_0^1 \dfrac{u(\tilde{x}_*, B(\tilde{x}_*))\,\mathrm{d}\xi}{\hat{B}(\beta^2 u(\tilde{x}_*, B(\tilde{x}_*))\xi, B(\tilde{x}_*))}, \\[3ex]
1 = \beta^2 \displaystyle\int_0^1 \dfrac{u^2(\tilde{x}_*, B(\tilde{x}_*))\,\xi\,\mathrm{d}\xi}{\hat{B}(\beta^2 u(\tilde{x}_*, B(\tilde{x}_*))\xi, B(\tilde{x}_*))}.
\end{cases}
\tag{37}
$$

In Section 4, we solve initial value problem (21)–(22) by using the finite-difference scheme.

4 Numerical results

4.1 The initial-value problem for KS and FB models

Problems (4) and (21)–(22) are nonlinear and no their analytical solutions could be derived. To solve these problems the finite-difference technique [32] was used. An implicit finite-difference schemes (see Appendix) were applied. The approximation resulted in the systems of linear algebraic equations with tridiagonal matrix which are solved effectively by using the elimination method [32]. To find a numerical solution the uniform discrete grids in space and time directions were introduced. The constant dimensionless steps of size 0.001 in space and time directions were used. The difference schemes preserve a discrete analogue of condition $\int_0^1 B(t,x)\,\mathrm{d}x = 1$. Digital experiments show that numerical solutions of both models for large time practically coincide with their exact steady-state solutions. The numerical experiments for different values of space and time steps show that the difference schemes are stable.

Numerical experiments performed for system (21)–(22) with $w_2(\Theta) = 1$, $x \in (0,1)$, show that, in the case of deep and some shallow layers, Θ becomes negative near the bottom of the chamber for small time, but later it becomes positive and tends to correct steady-state value as time grows. To preserve the positivity of Θ we used $w_2(\Theta) = 0$ for $x \in (0, x_*)$ and $w_2(\Theta) = 1$ for $x \in (x_*, 1)$. The similar scheme was used to solve system (4).

4.2 The steady-state Keller–Segel model

In the case of the shallow chamber, for fixed α and β, we determine $q = \alpha\beta^2/2$ and by Eq. (12) calculate β_*. Then, for $\beta < \beta_*$, to find ξ we solve Eq. (11) by splitting the interval in half. Knowing q and $\xi(q)$ we determine $B(0) = 2\alpha\xi^2/\beta^2$ and from Eqs. (9) and (10) find B and Θ for $x \in [0,1]$. Numerical results are demonstrated in Figs. 1–4 and Table 1.

In the deep layer case for fixed α and β, we calculate $\eta(\alpha)$, then, by Eqs. (17) and (18), determine x_*, $\tilde{\xi}$, and $B(x_*)$. Finally, by Eqs. (13) find $B(x)$ and $\Theta(x)$. Numerical results are exhibited in Figs. 5, 6 and Table 1.

4.3 The steady-state FB model

In the shallow chamber case, to determine $\tilde{B}(0)$, for fixed a_1 and a_2, we solve $(33)_2$ by splitting the interval in half. Knowing $\tilde{B}(0)$ we determine $\tilde{\beta}_*$ from Eq. $(33)_1$. Then by formula $B(0) = \tilde{\beta}_*\tilde{B}(0)$ we calculate $B(0)$. Now, from Eqs. (29) and (31) for given β and $B(0)$, we determine $x(\Theta')$ and $\Theta(\Theta')$ for $\Theta' \in [0, \beta^2]$. Results are exhibited in Figs. 1–4 and Table 2.

In the deep layer case, in order to determine $\tilde{x}_*$ and $B(\tilde{x}_*)$, for fixed β, a_1, and a_2, we solve system (37). This system is solved by determining numerically the point of the intersection of curves $(37)_1$ and $(37)_2$. Each curve we draw by determining $B(\tilde{x}_*)$ of argument $\tilde{x}_*$. To calculate $B(\tilde{x}_*)$ for a given $\tilde{x}_*$ we use a method of splitting the interval in half. Then, knowing $\tilde{x}_*$, β, $B(\tilde{x}_*)$, from Eq. (35) we determine $x(\Theta')$ and $\Theta(\Theta')$ for $\Theta' \in [0, \beta^2]$. At last, by Eq. (34), we calculate $B(x)$ for $x \in [0, \tilde{x}_*]$ and, for given γ, find v by equation $v = (1/\gamma)(a_2\Theta' - a_1 B)$, $x \in [0,1]$. Results are exhibited in Figs. 5, 6 and Table 2.

4.4 Analysis of the numerical results

The selection of parameters for numerical simulation approximately corresponds to the practically relevant values reported in the literature with the significant ranges in variation to allow demonstration of different regimes of microorganisms transport. We employ parameters that were used in the most calculations in [6,26,27]: $\kappa_1 = 2.12 \cdot 10^{-3}$ mm^2 s^{-3}, $\kappa_{20} = 10^5$ s^{-1}, $\kappa_{40} \in \left(1.3 \cdot 10^{-4}, 1.3 \cdot 10^{-3}\right)$ mm^2 s^{-1}, $B_0 = 10^5$ mm^{-3}, $C_0 = 1.5 \cdot 10^{14}$ mm^{-3}, $v_* = 7.4 \cdot 10^{-3}$ mm s^{-1}. In all calculations we used $\delta = 16.3$ and $\gamma = 460$.

Plots in Figs. 1–4 and 5, 6 depict the behaviour of bacteria and oxygen concentrations B and Θ for shallow and deep chambers, respectively.
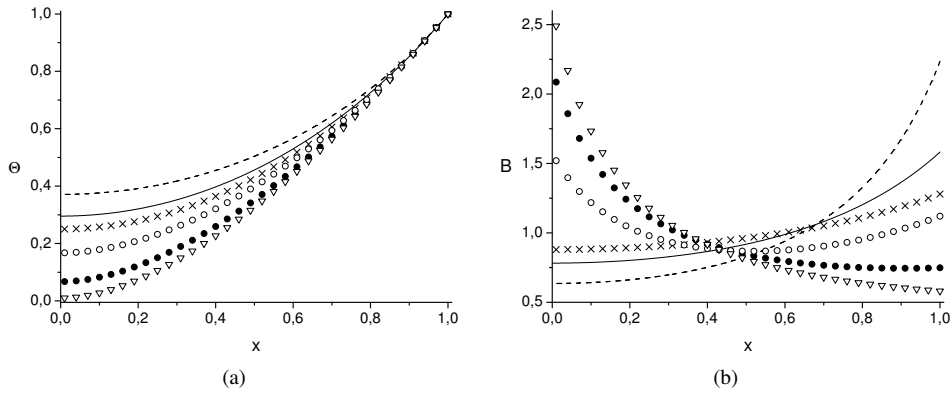

Fig. 1. The steady-state concentrations of the oxygen Θ (a) and bacterial cells B (b) versus x for the shallow layer in the case $a_1 = 2$ and $\beta^2 = 1.6$: $a_2 = \alpha = 0.5$ ($\triangledown$ FB model, $\times$ KS model), $a_2 = \alpha = 1$ ($\bullet$ FB model, — KS model), $a_2 = \alpha = 2$, $\beta_*^2 = 3.01$ ($\circ$ FB model, – – KS model).
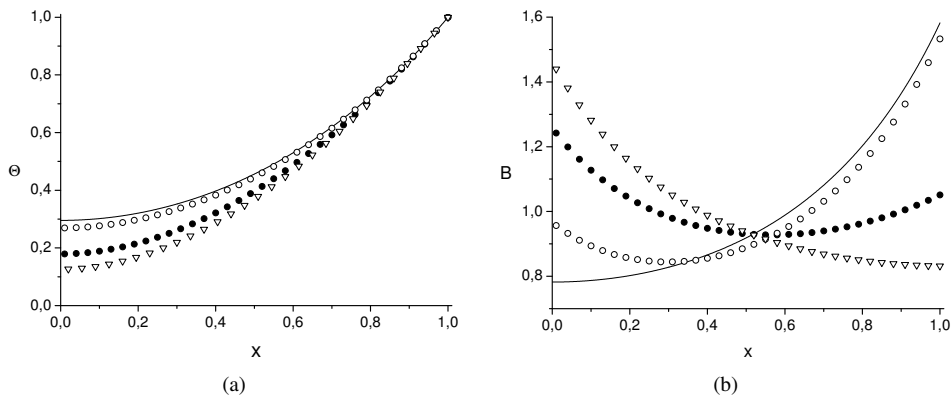

Fig. 2. Dependence of the steady-state Θ (a) and B (b) for the shallow layer on a_2 in the case $a_1 = 2$, $\alpha = 1$, $\beta^2 = 1.6$ at three values of a_2: 0.5 ($\triangledown$), 1 ($\bullet$), 2 ($\circ$)– $a_2 = 2$ FB model. Solid line for KS model.
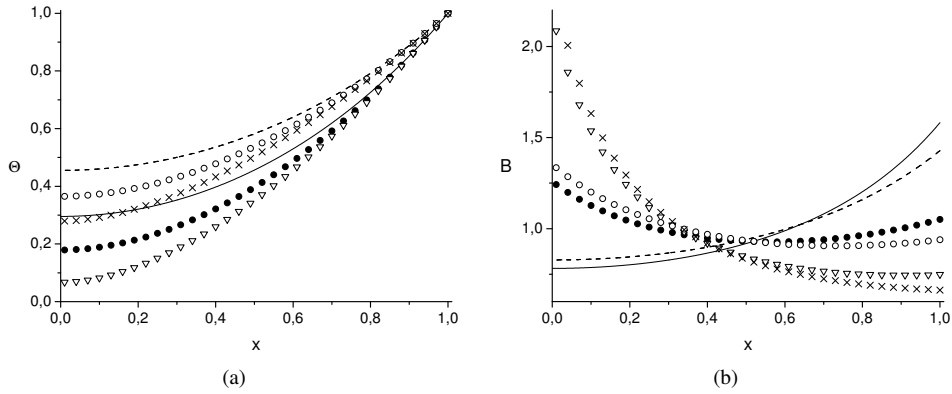
Fig. 3. Plot of steady-state Θ (a) and B (b) versus x for the shallow layer in the case $a_2 = \alpha = 1$. $\beta^2 = 1.6$ and a_1: 1 ($\bullet$), 2 ($\triangledown$) for FB model and solid line for KS model. $\beta^2 = 1.2$ and a_1: 1 ($\circ$), 2 ($\times$) for FB model and dashed line for KS model.
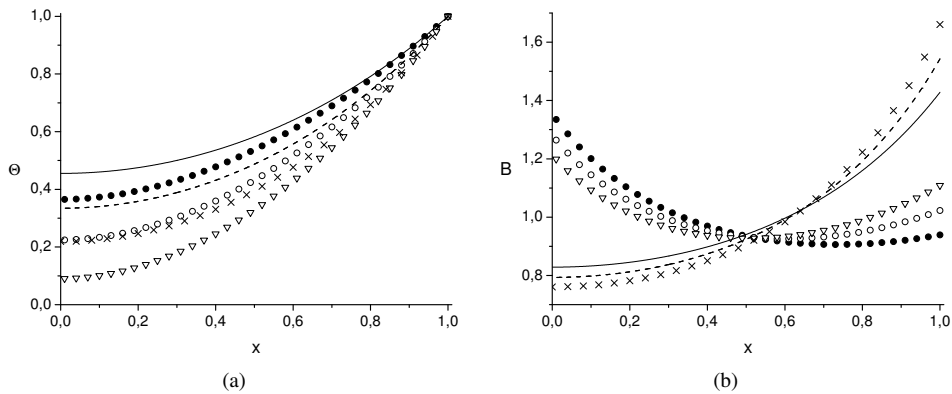

Fig. 4. The steady-state concentrations of the oxygen Θ (a) and bacterial cells B (b) versus x for the shallow layer in the case $a_1 = a_2 = \alpha = 1$ at three values of β^2: 1.2 ($\bullet$ FB model, — KS model), 1.5 ($\circ$ FB model, - - - KS model), 1.8 ($\triangledown$ FB model, $\times$ KS model).

Figs. 1(a) and 1(b) demonstrate a monotonic dependence of Θ and B for both KS and FB models on parameter $a_2 = \alpha$ for $a_1 = 2$, $\beta^2 = 1.6$. In the steady-state case, parameter $a_2 = \alpha$ characterizes a swimming upward velocity of microorganisms. Figs. 1(a) and 1(b) also illustrate a natural increase of Θ as a_2 grows and different behaviour of B near the bottom and the open surface. Concentration B decreases near the bottom and grows in a region of the open surface as a_2 increases. Moreover, B calculated from the FB model possesses a minimum value in the case where $a_1 = a_2 = \alpha = 2$ and $\beta^2 = 1.6$. B determined by KS model near the bottom is smaller than that calculated by FB model but near the open surface it behaves vice-versa. Oxygen concentration determined by KS model is greater than that calculated by FB one.
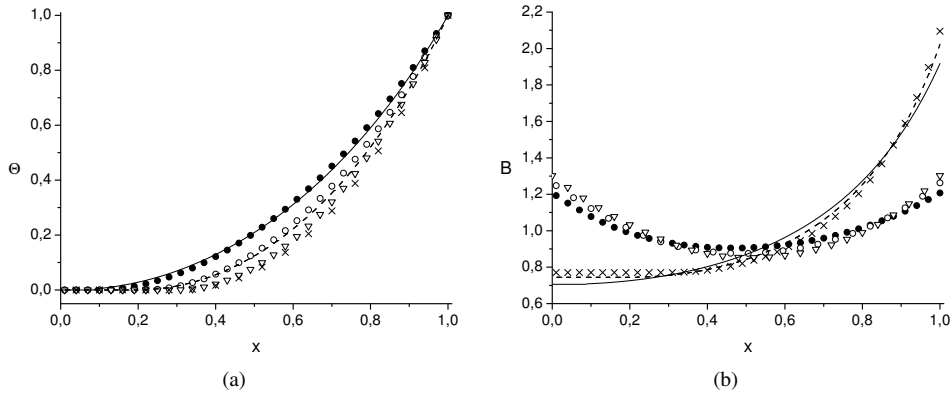
Fig. 5. The steady-state concentrations of the oxygen Θ (a) and bacterial cells B (b) versus x for the deep layer in the case $a_1 = a_2 = \alpha = 1$ at three values of β^2: 2.5 ($\bullet$ FB model, — KS model), 3.5 ($\circ$ FB model, - - - KS model), 4.5 ($\triangledown$ FB model, $\times$ KS model).
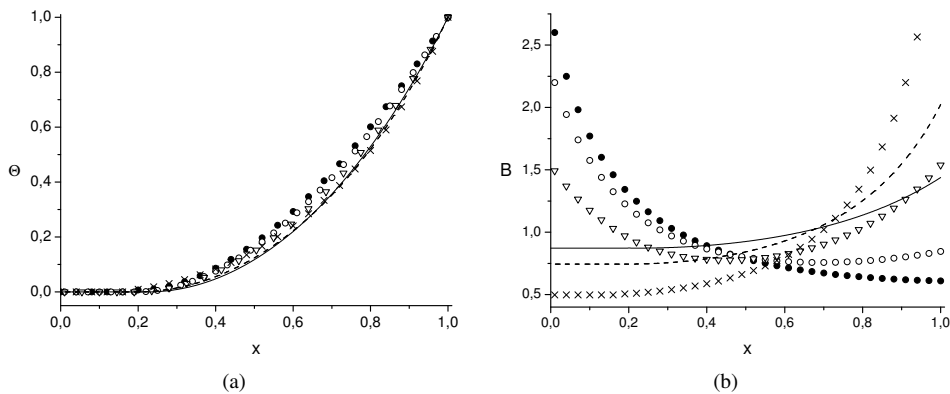

Fig. 6. Plots of the steady-state Θ (a) and B (b) versus x for the deep layer in the case $a_1 = 2$ and $\beta^2 = 3.5$: $a_2 = \alpha = 0.5$ ($\bullet$ FB model, — KS model), $a_2 = \alpha = 1$ ($\circ$ FB model, - - KS model), $a_2 = \alpha = 2$ ($\triangledown$ FB model, $\times$ KS model).

Figs. 2(a) and 2(b) illustrate the dependence of Θ and B on the parameter a_2 in the case $a_1 = \alpha = 1$ and $\beta^2 = 1.6$. Solid line depict Θ and B calculated by KS model. Curves of B corresponding to $a_2 = 1$ or $a_2 = 2$ possesses a minimum value which increases as a_2 decreases. Concentration Θ grows as a_2 increases but Θ determined by FB model is less than the oxygen concentration corresponding to KS one.

Plots in Figs. 3(a) and 3(b) depict the dependence of Θ and B on parameters a_1 and β^2 for FB model and on parameter β^2 for KS model. Note that parameters a_1 and β^2 characterize an influence of gravity and a chamber depth. Curves demonstrate the different behaviour of B in a region of the bottom and open surface. Near the bottom B grows

as a_1 increases but far from the bottom it behaves vice-versa. Figure also demonstrates the different behaviour of B determined by both KS and FB models. Oxygen concentration Θ decreases for all x as a_1 or β^2 increases.

Plots in Figs. 4(a) and 4(b) depict the dependence of Θ and B on parameter β^2 for both KS and FB models and demonstrate their monotonic behaviour as β^2 grows. Values of B that correspond to KS and FB models near the bottom are larger than corresponding ones near the open surface. Values of Θ determined by KS model for all x are larger that those corresponding with FB model.

Figs. 5(a) and 5(b), 6(a) and 6(b) demonstrate the dependence of Θ and B on parameters β^2 and a_2, respectively, for a deep chamber. We observe a monotonic behaviour of B for both KS and FB models with respect to parameter β^2. But this behaviour is similar near the bottom and the open surface and is different in the intermediate region (see Figs. 5(a) and 5(b)). The qualitative behaviour of B and Θ with respect to a_2 is similar to that of the shallow chamber (see Figs. 6(a) and 6(b)).

Table 1 demonstrates the dependence of $\tilde{\beta}_*^2$ on parameters a_1, a_2 and $\tilde{x}_*$, $B(\tilde{x}_*)$ on β^2 from steady-state FB model. Parameter $\tilde{\beta}_*^2$ decreases as a_1 grows and increases with a_2 increasing. For the deep chamber case $\tilde{x}_*$, $B(\tilde{x}_*)$ grow as β^2 increases. Table 2 demonstrates the similar behaviour of β_*^2, x_* and $B(x_*)$ for steady state case of KS model.

Fig. 7 demonstrates the comparison of the behaviour of B determined by the KS and FB models for the shallow chamber in the time-dependent case. For small time and $v_0 = 0.01$, we observe near the top and bottom a non-monotonic behaviour of B determined by the FB model. For fixed x, B reaches a maximum value and then tends to an asymptotic one as time increases. We also observe a small maximum value of B determined by the KS mode l for small time at $x = 1$. In the top region, Figs. 7(a) and 7(b) demonstrate a different behaviour of B determined by KS and FB models as the depth of the chamber, β^2, grows. From Fig. 7(a) for small time and $\beta^2 = 5$, we can see that B determined by the FB model in the top region is larger than that determined by the KS one, while Fig. 7(b) depicts the vice-versa behaviour of B for $\beta^2 = 2$. Numerical experiments reveal a similar qualitative behaviour of B for the deep chamber as well.

Table 1. Parameters of the KS model.

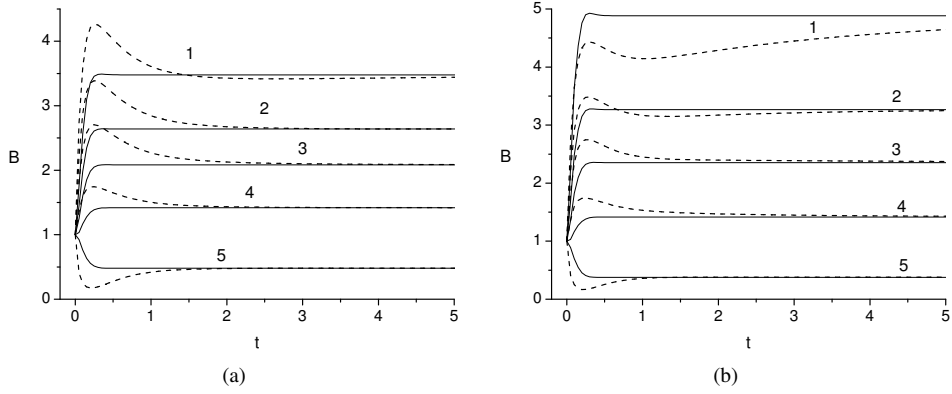| α	β_*^2	β^2	x_*	$B(x_*)$
0.5	2.18	2.5	0.071	0.851
		3.5	0.224	0.873
		4.5	0.321	0.887
1	2.41	2.5	0.021	0.706
		3.5	0.195	0.745
		4.5	0.302	0.771
2	3.02	3.5	0.095	0.497
		4.5	0.233	0.539
5	7.23	7.5	0.032	0.126
		8.5	0.133	0.139
		10	0.248	0.157

Fig. 7. Comparison of B for time-dependent KS (Eq. (4)) and FB (Eqs. (21), (22) with $v_0 = 0.01$) models for fixed values of x: 1 (1), 0.95 (2), 0.9 (3), 0.8 (4) 0.1 (5) in the case where $a_1 = 0.001$, $a_2 = \alpha = 3$, $\tilde{\beta}_*^2 = 3.9195$, $\beta_*^2 = 3.9186$. (a) $\beta^2 = 2$, (b) $\beta^2 = 3$. — KS model, - - - FB model.

Table 2. Parameters of the FB model.

a_1	a_2	$\tilde{\beta}_*^2$	β^2	$\tilde{x}_*$	$B(\tilde{x}_*)$
0.01	1	2.40	2.5	0.022	0.709
			3.5	0.195	0.747
			5	0.342	0.783
0.01	5	7.21	7.5	0.035	0.127
			8.5	0.135	0.140
			10	0.249	0.157
0.1	1	2.36	2.5	0.032	0.741
			3.5	0.199	0.770
			5	0.343	0.798
0.1	5	7.02	7.5	0.056	0.134
			8.5	0.154	0.147
			10	0.264	0.165
1	0.5	1.85	2.5	0.110	1.254
			3.5	0.224	1.116
			4.5	0.302	1.037
1	1	2.01	2.5	0.089	1.091
			3.5	0.214	0.995
			4.5	0.297	0.939
1	2	2.44	3.5	0.170	0.743
			4.5	0.271	0.730
2	0.5	1.62	3.5	0.199	1.312
2	1	1.73	3.5	0.197	1.205
2	2	2.04	3.5	0.186	0.978

Fig. 8 demonstrates the influence of the initial value v_0 on the behaviour of B determined by the FB model. B is monotonic in time for $v_0 < 0.007$, but it is non-monotonic if $v_0 > 0.007$.
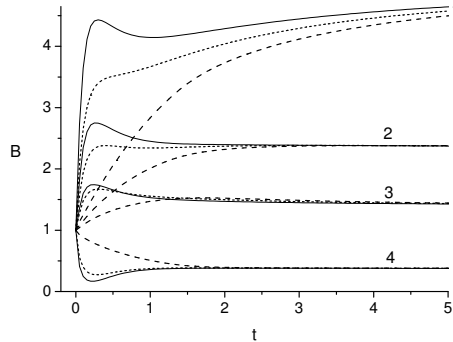

Fig. 8. Effect of v_0 on cells concentration B determined by time-dependent FB model (21) and (22) at $a_1 = 0.001$, $a_2 = 3$, $\tilde{\beta}_*^2 = 3.9195$, $\beta^2 = 3$ for fixed values of x: 1 (1), 0.9 (2), 0.8 (3), 0.1 (4). Values of v_0: — 0.01, $\cdots$ 0.007, - - - 0.001.

5   Concluding remarks

In this paper we studied the steady-state and the initial value problems for oxytactic swimming upwardly bacteria using the modified Keller–Segel model termed FB model. It includes the conservation equations for the oxygen and cells concentrations and the additional one for the balance of forces acting on bacteria (momentum equation for cells). Differently from the KS model, the thrust force, but not the average cells velocity, is approximated by the term proportional to the oxygen gradient.

The steady-state solution of the FB model is given analytically and studied numerically but the initial value problem is studied only numerically. In the deep layer case near the bottom the oxygen concentration is insufficient for cells to be active. In this region we only excluded the oxygen consumption and used the continuity conditions for concentrations and their derivatives at the point where $\Theta = 0$. Above this point Θ is positive.

We studied difference between solutions of the the KS and FB models and found that in the steady-state case because of gravity the FB model determines more slow swimming upwards of the oxytactic cells comparing with that determined by the KS one. This means that oxygen consumption time grows and, hence, the oxygen concentration decreases since its diffusion is a slow process. This leads to the increase of cells concentration near the bottom and its decrease at the top of the chamber. In the case of small difference of bacteria and fluid densities, asymptotic in time values of B for the KS and FB models practically coincide.

In the time-dependent problem the transition period after the initial moment of the concentrations B and Θ (the cells adaptation period) determined by the KS model is shorter than the corresponding one determined by the FB model.

We hope that the model of the FB type with an additional term of bacteria to bacteria communication in the differential equation for v could be regarded as phenomenological effective one to capture the possible variability of the oxytactic bacteria response to the environmental changes in real systems.

Appendix

To find the numerical solution of problem (21) and (22) the finite-difference scheme was used.

Assume that $t_j = j\tau$, $0 \leqslant j \leqslant M$, $\tau = T/M$, $x_i = ih$, $0 \leqslant i \leqslant N$, $h = 1/N$. Set $\theta_i^j = \theta(t_j, x_i)$, $b_i^j = b(t_j, x_i)$, $v_i^j = v(t_j, x_i)$.

Approximating the differential equations (21) with an implicit scheme the following finite difference equations are obtained:

$$
\begin{cases}
\dfrac{\theta_i^{j+1} - \theta_i^j}{\tau} = \delta\left(\dfrac{\theta_{i-1}^{j+1} - 2\theta_i^{j+1} + \theta_{i+1}^{j+1}}{h^2} - \beta^2 b_i^j\right), \\[3mm]
\dfrac{b_i^{j+1} - b_i^j}{\tau} = \dfrac{b_{i-1}^{j+1} - 2b_i^{j+1} + b_{i+1}^{j+1}}{h^2} - \gamma\dfrac{v_{i+1}^j b_{i+1}^j - v_{i-1}^j b_{i-1}^j}{2h}, \\[3mm]
b_i^j \dfrac{v_i^{j+1} - v_i^j}{\tau} = \dfrac{\rho_3}{\gamma}\left(-a_1 b_i^j + a_2 \dfrac{\theta_{i+1}^j - \theta_{i-1}^j}{2h} - \gamma v_i^j\right), \\[3mm]
i = 1, 2, \ldots, N-1;\ j = 0, 1, \ldots, M-1.
\end{cases}
\tag{A.1}
$$

The boundary and initial conditions (22) are approximated by

$$
\begin{cases}
\dfrac{b_1^{j+1} - b_0^{j+1}}{h} - \gamma\dfrac{v_1^j b_1^j + v_0^j b_0^j}{2} = 0, \\[3mm]
\dfrac{b_N^{j+1} - b_{N-1}^{j+1}}{h} - \gamma\dfrac{v_{N-1}^j b_{N-1}^j + v_N^j b_N^j}{2} = 0, \\[3mm]
\theta_1^{j+1} = \theta_0^{j+1}, \quad \theta_N^{j+1} = 1, \\[2mm]
\theta_i^0 = 1, \quad b_i^0 = 1, \quad v_i^0 = v_0, \\[2mm]
i = 0, 1, \ldots, N;\ j = 0, 1, \ldots, M-1.
\end{cases}
\tag{A.2}
$$

To get the discrete form of Eq. $(21)_3$ at $x = 0$ and 1 we use the difference equations

$$
\begin{cases}
b_0^j \dfrac{v_0^{j+1} - v_0^j}{\tau} = \dfrac{\rho_3}{\gamma}\left(-a_1 b_0^j - \gamma v_0^j\right), \\[3mm]
b_N^j \dfrac{v_N^{j+1} - v_N^j}{\tau} = \dfrac{\rho_3}{\gamma}\left(-a_1 b_N^j + a_2 \dfrac{\theta_N^j - \theta_{N-1}^j}{h} - \gamma v_N^j\right), \\[3mm]
j = 0, 1, \ldots, M-1.
\end{cases}
\tag{A.3}
$$

To write the difference scheme to KS model the following approximation of $(4)_2$ and boundary conditions for function B instead of Eqs. $(A.1)_2$ and $(A.2)_{1,2}$ are used:

$$\begin{cases} \dfrac{b_i^{j+1} - b_i^j}{\tau} = \dfrac{b_{i-1}^{j+1} - 2b_i^{j+1} + b_{i+1}^{j+1}}{h^2} \\[2mm] \quad - \dfrac{\alpha}{h}\left(\dfrac{b_{i+1}^j + b_i^j}{2}\dfrac{\theta_{i+1}^j - \theta_i^j}{h} - \dfrac{b_i^j + b_{i-1}^j}{2}\dfrac{\theta_i^j - \theta_{i-1}^j}{h} \right), \\[2mm] i = 1, 2, \ldots, N-1; \ j = 0, 1, \ldots, M-1, \end{cases} \tag{A.4}$$

$$\begin{cases} b_1^{j+1} = b_0^{j+1}, \\[2mm] \dfrac{b_N^{j+1} - b_{N-1}^j}{h} - \alpha\dfrac{b_{N-1}^j + b_N^j}{2}\dfrac{\theta_N^j - \theta_{N-1}^j}{h} = 0, \\[2mm] j = 0, 1, \ldots, M-1. \end{cases} \tag{A.5}$$

From $(A.1)_2$, $(A.2)_{1,2}$ or $(A.4)$, $(A.5)$ the discrete analogue of condition (6) $h\sum_{i=1}^{N-1} b_i^{j+1} = h\sum_{i=1}^{N-1} b_i^j$, $j = 0, 1, \ldots, M-1$, follows.

References

1. E.F. Keller, L.A. Segel, Model for chemotaxis, *J. Theor. Biol.*, **30**:225–234, 1971.

2. E.F. Keller, L.A. Segel, Travelling bands of chemotaxis bacteria, *J. Theor. Biol.*, **30**:235–248, 1971.

3. D. Horstmann, From 1970 until present: The Keller–Segel model in chemotaxis and its consequences. I, *Jahresberichte DMV*, **105**(3):103–165, 2003.

4. T. Hillen, K.J. Painter, A user's guide to PDE models for chemotaxis, *J. Math. Biol.*, **58**:183–217, 2009.

5. N.A. Hill, T.J. Pedley, Bioconvection, *Fluid Dyn. Res.*, **37**:1–20, 2005.

6. A.J. Hillesdon, T.J. Pedley, J.O. Kessler, The development of concentration gradients in a suspension of chemotactic bacteria, *Bull. Math. Biol.*, **57**(2):299–344, 1995.

7. A.J. Hillesdon, T.J. Pedley, Bioconvection in suspensions of oxytactic bacteria: Linear theory, *J. Fluid Mech.*, **324**:223–259, 1996.

8. C. Dombrowski, L. Cisneros, S. Shatkaew, R. Goldstein, J. Kessler, Self-concentration and large-scale coherence in bacterial dynamics, *Phys. Rev. Lett.*, **93**, 098103, 2004.

9. I. Tuval, L. Cisneros, C. Dombrowski, C. Wolgemuth, J. Kessler, R. Goldstein, Bacterial swimming and oxygen transport near contact lines, *Proc. Natl Acad. Sci.*, **102**:2277–2282, 2005.

10. A. Chertock, K. Fellner, A. Kurganov, A. Lorz, P.A. Markowich, Sinking, merging and stationary plumes in a coupled chemotaxis-fluid model: A high-resolution numerical approach, *J. Fluid Mech.*, **694**:155–190, 2012.

11. A. Lorz, Coupled chenmotaxis fluid model, *Math. Models Meth. Appl. Sci.*, **20**:1–17, 2010.

12. R.-J. Duan, A. Lorz, P. Markovich, Global solutions to the coupled chemotaxis-fluid equations, *Commun. Part. Diff. Equ.*, **35**:1–39, 2010.

13. M. Di Francesco, A. Lorz, P. Markovich, Chemotaxis-fluid coupled model for swimming bacteria with nonlinear diffusion: Global existence and asymptotic behaviour, *Discrete Contin. Dyn. Syst. A*, **28**(4):1437–1453, 2010.

14. S.M. Becker, A.V. Kuznetsov, A.A. Avramenko, Numerical modelling of a falling bioconvection plume in a porous medium, *Fluid Dyn. Res.*, **33**:323–339, 2004.

15. A.V. Kuznetsov, A.A. Avramenko, Analysis of stability of bioconvection of motile oxytactic bacteria in a horizontal fluid saturated porous layer, *Int. Commun. Heat Mass Transfer*, **30**:593–602, 2003.

16. A.V. Kuznetsov, A.A. Avramenko, P. Geng, Analytical investigation of a falling plume caused by bioconvection of oxytactic bacteria in a fluid saturated porous medium, *Int. J. Eng. Sci.*, **42**:557–569, 2004.

17. A.V. Kuznetsov, Thermo-bioconvection in a suspension of oxytactic bacteria, *Int. Commun. Heat Mass Transfer*, **32**:991–999, 2005.

18. A.V. Kuznetsov, Investigation of the onset of thermo-bioconvection in a suspension of oxytactic microorganisms in a shallow fluid layer heated from below, *Theor. Comput. Fluid. Dyn.*, **19**(4):287–299, 2005.

19. A.V. Kuznetsov, The onset of thermo-bioconvection in a shallow fluid saturated porous layer heated from below in a suspension of oxytactic microorganisms, *Eur. J. Mech. B Fluids*, **25**:223–233, 2006.

20. Z. Alloui, T.H. Nguyen, E. Bilgen, Bioconvection of gravitactic microorganisms in a vertical cylinder, *Int. J. Heat Mass Transfer*, **32**:739–747, 2005.

21. Z. Alloui, T.H. Nguyen, E. Bilgen, Numerical investigation of thermo-bioconvection in a suspension of gravitactic microorganisms, *Int. J. Heat Mass Transfer*, **50**:1435–1441, 2007.

22. Z. Alloui, T.H. Nguyen, E. Bilgen, Stability analysis of thermo-bioconvection in suspensions of gravitactic microorganisms in a fluid layer, *Int. Commun. Heat Mass Transfer*, **33**:1198–1206, 2006.

23. M.A. Herrero, J.J.L. Velazquez, Chemotactic collapse for the Keller–Segel model, *J. Math. Biol.*, **35**:177–194, 1996.

24. B.L. Taylor, I.B. Zhulin, M.S. Johnson, Aerotaxis and other energy sensing behavior in bacteria, *Ann. Rev. Microbiol.*, **53**:103–128, 1999.

25. J. Shioi, C.V. Dang, B.L. Taylor, Oxygen as attractant and repellent in bacterial chemotaxis, *J. Bacteriol.*, **169**(7):3118–3123, 1987.

26. R. Baronas, R. Šimkus, Modeling the bacterial self-organization in a circular container along the contact line as detected by bioluminescence imaging, *Nonlinear Anal. Model. Control*, **16**(3):270–282, 2011.

27. R. Šimkus, R. Baronas, Metabolic self-organization of bioluminescent *Escherichia coli*, *Luminescence*, **26**(6):716–721, 2011.

28. M. Eisenbach, *Chemotaxis*, Imperial College Press, London, 2004.

29. R.M. Macnab, D.E. Koshland, Jr., The gradient-sensing mechanism in bacerial chemotaxis, *Proc. Nat. Acad. Sci. USA*, **69**(9):2509–2512, 1972.

30. H.G. Othmer, T. Hillen, The diffusion limit of transport equations II: Chemotaxis equations, S*IAM J. Appl. Math.*, **62**(4):1222–1250, 2002.

31. T. Hillen, K. Painter, C. Schmeiser, Global existence for chemotaxis with finite sampling radius, *Discr. Cont. Dyn. Syst. B*, **7**(1):125–144, 2007.

32. A.A. Samarskii, *The Theory of Difference Schemes*, Marcel Dekker, New York, 2001.